1980ApJ...240..871S

THE ASTROPHYSICAL JOURNAL, 240:871–884, 1980 September 15
© 1980. The American Astronomical Society. All rights reserved. Printed in U.S.A.

VV PUPPIS AND AN URSAE MAJORIS: A RADIAL VELOCITY STUDY

DONALD P. SCHNEIDER AND PETER YOUNG
Palomar Observatory, California Institute of Technology
Received 1980 February 4; accepted 1980 March 31

ABSTRACT

The emission lines of VV Puppis and AN Ursae Majoris have been observed through complete orbits at 2 Å spectral and 5 minutes temporal resolution.

VV Puppis exhibits spectacular emission line variations. The lines have a mean radial velocity amplitude $K = 376$ km s^{-1} and have clearly defined broad and sharp components. The sharp component becomes very strong when maximally redshifted ($+450$ km s^{-1}) and remains strong while moving to its maximum blueshift (-450 km s^{-1}), then suddenly becomes weak. Its movement lags the broad pedestal of emission on which it is superposed by 55° in phase.

AN UMa exhibits similar but less spectacular variations. The mean radial velocity amplitude $K = 256$ km s^{-1} and the base and peak of the emission lines are 49° out of phase. A milder version of the sharp component effect is seen in this system.

Attempts are made to integrate particle trajectories in the Roche geometry where a dipole magnetic field dominates the gas flow. The results seem to support the idea that gas is threaded on the magnetic field near the L_1 point whence it free-falls onto the favorably oriented magnetic pole of the white dwarf. Broad line emission would arise from gas plunging down the accretion column, and sharp line emission either from gas near the L_1 point or a red dwarf star irradiated by UV light.

Subject headings: stars: binaries — stars: individual — stars: magnetic

I. INTRODUCTION

VV Puppis and AN Ursae Majoris are both members of the class of AM Herculis magnetic binary systems. These systems resemble nonmagnetic cataclysmic binaries but are distinguishable from those systems by virtue of strong ($\sim 10\%$) continuum circular polarization, and also because of their high excitation emission line spectra.

Both VV Pup and AN UMa were considered to be cataclysmic variables prior to 1977; VV Pup in particular has a voluminous photometric and spectroscopic history. VV Pup was recognized as a magnetic binary by Tapia (1977*b*) from its strong circular polarization. AN UMa was classified both from its spectral peculiarities (Bond and Wagner 1977), and from its circular polarization (Krzeminski and Serkowski 1977).

Radial velocity studies of AM Herculis (Greenstein *et al.* 1977; Young and Schneider 1979) have shown somewhat bizarre behavior in the emission and absorption lines. An emission line study of another magnetic binary (2A 0311−227) by Schneider and Young (1980; hereafter SY) also showed curious behavior. The emission line radial velocity variations ($K \sim 350$ km s^{-1}) in both binaries appear to reflect not orbital motion but rather a streaming of gas threaded on the magnetic field lines generated by the white dwarf in the system.

Both VV Pup and AN UMa have been subjected to spectroscopic study (in Herbig 1960 and Tapia 1977*a*, respectively). In this study we observed both objects with a spectral resolution of 2 Å and a time resolution of about 5 minutes. This is sufficient to show that both binaries exhibit the strange emission line contortions that characterize AM Her and 2A 0311−227.

In § II we discuss the observations, in §§ III and IV we analyze the data for VV Pup and AN UMa, and in § V we discuss the observations with the aid of some models.

II. OBSERVATIONS

a) Instrumentation

On two nights in 1979 December we examined VV Pup and AN UMa, covering 1.5 and 2 orbital periods, respectively (the periods being 1.674 and 1.914 hours). The Journal of Observations is given in Table 1.

The 200 inch (5.1 m) Hale telescope equipped with the digital SIT spectrograph was used to monitor the systems. At the Cassegrain focus we used a 0.″9 by 61″ slit and a dispersion of 73 Å mm^{-1} to give a resolution of 2.1 Å for most of the observations. A flux measurement on each object was made using twin 8″ diameter apertures. As usual, integration times (200 s on VV Pup; 400 s on AN UMa) were a compromise between using the instrument efficiently (it has a "dead time" of 114 s between exposures) and keeping the charge level on the SIT low (to minimize beam bending). The 512 pixels in the wavelength direction ran from 4250 to 4940 Å, and the data were mildly undersampled (arc lines having an FWHM of 1.6 pixels).

© American Astronomical Society • Provided by the NASA Astrophysics Data System

1980ApJ...240..871S

TABLE 1

JOURNAL OF OBSERVATIONS

Object	Date and Time (UT) 1979 Dec.	Aperture	Int. Time (s)	Number of Integrations	Number of Orbits
VV Pup	10.334–10.432	0.″9 × 61″ slit	200	26	1.41
VV Pup	10.434–10.441	8″ diam. hole	200	2	0.10
AN UMa	10.455–10.467	8″ diam. hole	300	2	0.15
AN UMa	10.469–10.567	0.″9 × 61″ slit	400	17	1.23
AN UMa	11.485–11.563	0.″9 × 61″ slit	400	13	0.98

Inert gas He-Ne-A spectra were taken to calibrate the wavelength scale; spectrophotometric standard stars established the flux scale for the 8″ aperture observations.

b) *The Data*

In Figure 1 we show data averaged over one orbit for both VV Pup and AN UMa (where more than one orbit was observed, we have taken observations for the first 1.00 orbits only). This includes slit observations only, and the data were shifted into the rest frame of the moving emission lines before averaging them.

The spectra bear a strong resemblance to those of AM Her (Stockman *et al.* 1977) and 2A 0311−227 (SY) in the detailed appearance of the emission lines. Equivalent widths for the various lines averaged over an orbit are given in Table 2. Among the features shared by all four known magnetic binaries are:

1. *A low Balmer decrement.* Generally Hβ or Hγ is the strongest Balmer line. The FWHM of the Balmer lines is 800–850 km s^{-1} (although for 2A 0311−227 it is somewhat higher at 1100 km s^{-1}).

2. *Strong* He II λ4686 *emission.* This has an FWHM slightly (but significantly) smaller than of the Balmer lines, at ∼725 km s^{-1} (again 2A 0311−227 has slightly fatter lines).

In Figure 2 the flux calibrated spectra for VV Pup and AN UMa are shown. As is usual for magnetic binaries, the f_ν for the continuum is almost flat, rising slightly in the red.

III. VV PUPPIS

a) *The Period*

The ephemeris given by Walker (1965) for photometric maximum is

$$\mathrm{HJD} = 2427889.6474 + 0.0697468256E\,. \quad (1)$$

In Figure 3 we show our photometry through a 0.″9 slit in the form of a light curve. It is relevant to note that Warner and Nather (1972) found the eclipse ingress to be very rapid and to be centered on phase $\phi = 0.17$ (all phases defined in this paper for VV Pup will be derived from eq. [1]). There is therefore no evidence for a gross error in the ephemeris (1).

Spectroscopic observations will provide better fiducial points from which to obtain a period. The data of Herbig (1960) showed a radial velocity curve with an

TABLE 2

EMISSION LINES IN VV PUPPIS AND AN URSAE MAJORIS

Line	VV Puppis[a] Eq. Width (Å)	VV Puppis[a] FWHM (km s^{-1})	AN Ursae Majoris[b] Eq. Width (Å)	AN Ursae Majoris[b] FWHM (km s^{-1})
C II λ4267	1.7	...	0.4	...
Hγ	42.5	780	13.8	780
He I λ4388	2.7	790	1.2	730
O II λ4416 + Fe III λ4419	0.8	...	0.6	...
He I λ4471	12.0	820	4.6	790
He II λ4541	1.6	...	...	...
N III λ4640 + C III λ4647	9.0	...	2.7	...
He II λ4686	43.4	730	13.7	720
He I λ4713	2.4	...	1.2	...
Hβ	50.3	810	18.9	810
He I λ4921	4.9	750	2.6	750

[a] Mean values over one orbit. The mean continuum level over this orbit was $AB_\nu = 15.08$ (virtually constant with wavelength).

[b] Mean values over one orbit with mean continuum level at $AB_\nu = 16.19$.

© American Astronomical Society • Provided by the NASA Astrophysics Data System

1980ApJ...240..871S

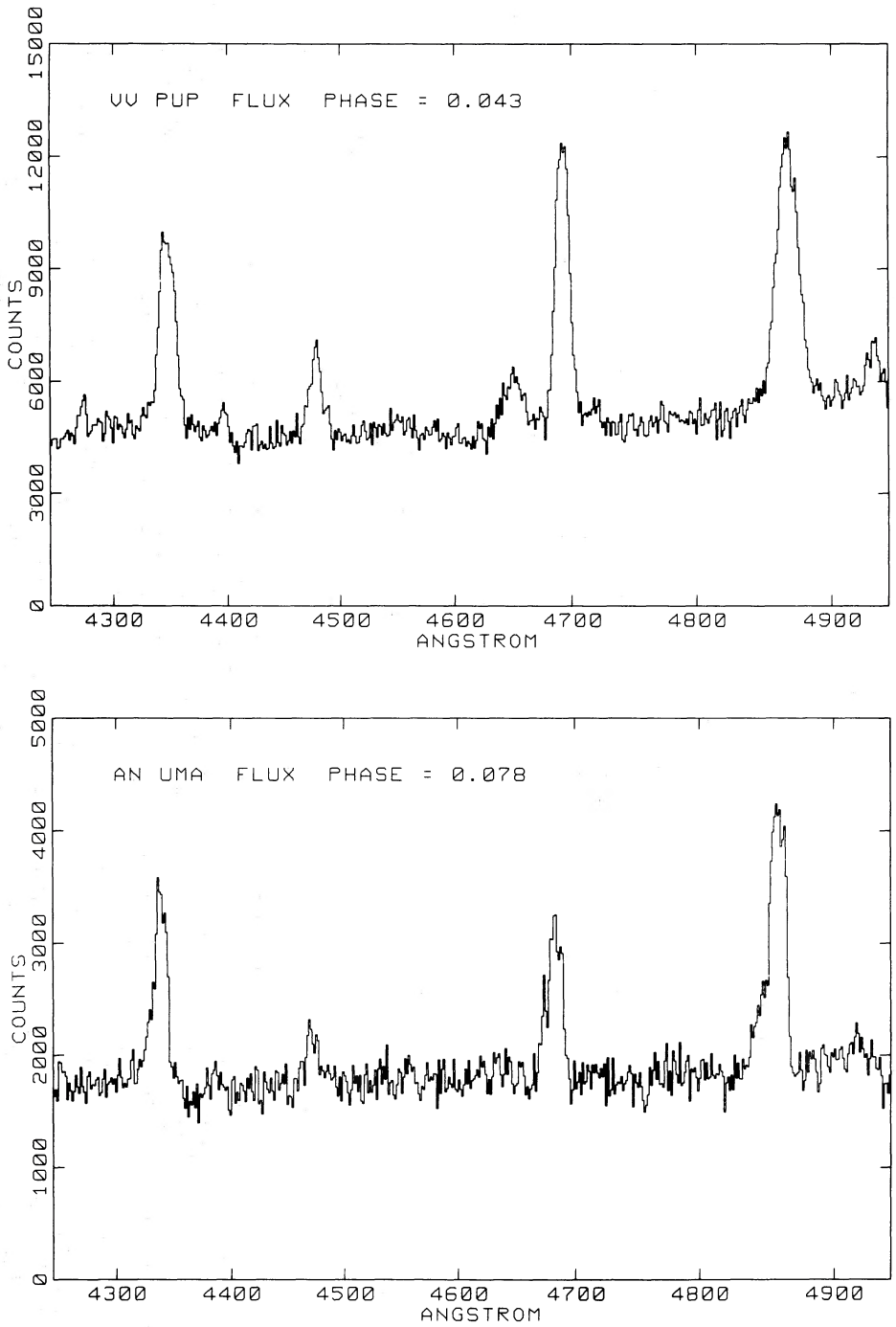

FIG. 2.—Flux-calibrated spectra of VV Pup and AN UMa. One data number corresponds to $AB_v = 24.0$; the data are on a linear scale. The orbital phase of each observation is given in the figure. The spectral resolution was defined by the seeing disk and is estimated to be 3 Å.

© American Astronomical Society • Provided by the NASA Astrophysics Data System

1980ApJ...240..871S

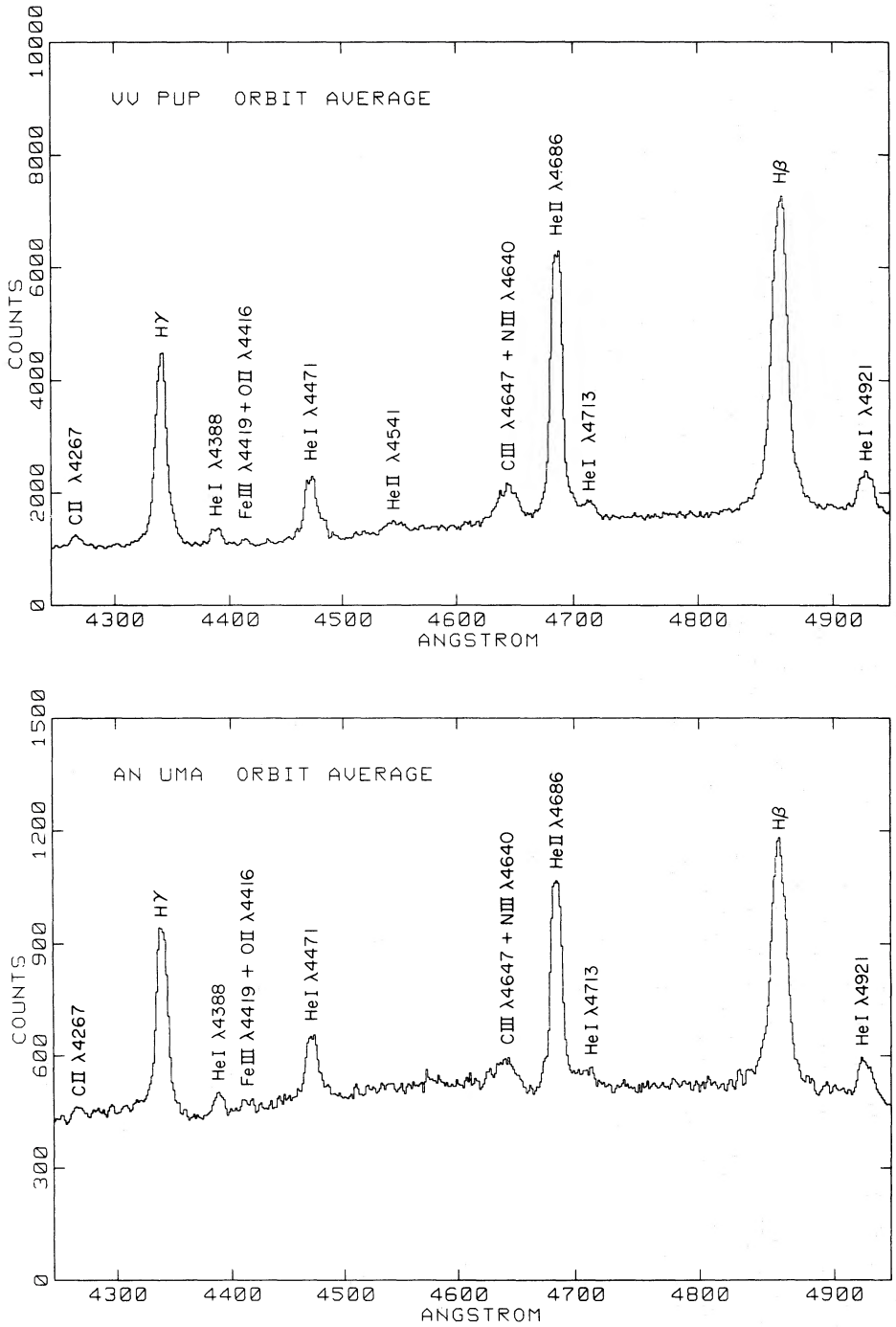

FIG. 1.—Orbit-averaged spectra of VV Pup and AN UMa. The spectral resolution is 2.1 Å, and the data are not flux calibrated (although the relative calibration is reasonably good). The major emission lines are labeled. Data were shifted into rest frame of emission lines prior to summation.

© American Astronomical Society • Provided by the NASA Astrophysics Data System

1980ApJ...240..871S

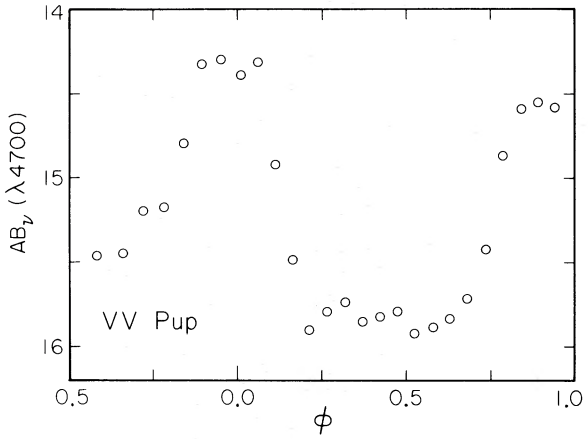

FIG. 3.—Light curve of VV Pup from Cassegrain slit photometry. The curve has been normalized with a total flux observation to give AB_v at λ4700. Photometric phase ϕ from the standard ephemeris is the abscissa.

elliptical orbit $e = 0.087$. The apparent ellipticity is due to the interplay of two components in the emission lines, as we shall see below. In order to provide a fiducial point directly comparable with ours, the data of Herbig (1960) were fitted with a circular orbit. The results are in Table 3. The notation is defined by the velocity curve

$$V = \gamma + K \sin(\phi - \phi_0) . \quad (2)$$

From this fit we obtain an epoch for the mean lines having $V = \gamma$ and crossing from blue to red of

$$\text{HJD} = 2436550.02610 \pm 0.00080 , \quad (3)$$

for Herbig's data.

In order to simulate this in our own data, we have determined radial velocities for the mean position of the four strongest lines in our wavelength interval. The results are given in Table 3. The K-value is smaller than that derived by Herbig (1960), but all four lines agree well. The state of the γ-velocity is most satisfactory and shows that we have been successful in keeping beam-bending effects in the SIT detector small. Our epoch for line crossing is

$$\text{HJD} = 2444217.92469 \pm 0.00034 . \quad (4)$$

Inspection of the ϕ_0 values in Table 3 shows only a very slight drift of the ephemeris (1) at the current epoch. The period we derive is (correcting into ephemeris time)

$$P = 0^d.0697468487 \pm 0.0000000079 . \quad (5)$$

The period of Walker (1965) differs by only 3 σ from this; we shall continue to give phases from equation (1).

b) *Emission Line Behavior*

Figure 4 shows 19 observations of VV Pup covering an entire orbit. In Figure 5 we present Boroson-Greenstein diagrams for the He II λ4686 and Hβ lines (such diagrams for AM Her were given by Greenstein *et al.* [1977]).

The most striking feature is the appearance of a sharp component in emission at $\phi = 0.1$. This is initially seen redshifted but executes a sharp move to the blue and finally disappears at $\phi = 0.7$. This component, weakly visible at other phases, is out of

TABLE 3

RADIAL VELOCITIES IN VV PUPPIS

Line[a]	K (km s^{-1})	γ (km s^{-1})	ϕ_0	$\sigma(O-E)$ (km s^{-1})
Mean[b]	426 ± 31	66 ± 23	0.787 ± 0.012	123
Hγ	380 ± 22	77 ± 16	0.816 ± 0.009	76
He I λ4471	372 ± 21	68 ± 15	0.819 ± 0.009	73
He II λ4686	366 ± 15	41 ± 11	0.834 ± 0.007	53
Hβ	385 ± 21	53 ± 15	0.809 ± 0.008	72
Mean	376 ± 10	60 ± 8	0.820 ± 0.005	...
Hγ (S)	443 ± 18	3 ± 13	0.862 ± 0.006	62
He I λ4471 (S)	398 ± 19	0 ± 15	0.877 ± 0.006	64
He II λ4686 (S)	468 ± 17	14 ± 13	0.877 ± 0.006	61
Hβ (S)	439 ± 20	45 ± 14	0.867 ± 0.007	67
Mean (S)	437 ± 15	16 ± 10	0.871 ± 0.003	...
Hγ (B)	436 ± 23	40 ± 16	0.729 ± 0.008	80
He I λ4471 (B)	514 ± 20	74 ± 13	0.735 ± 0.010	66
He II λ4686 (B)	504 ± 21	52 ± 15	0.719 ± 0.006	73
Hβ (B)	496 ± 15	56 ± 11	0.718 ± 0.005	53
Mean (B)	488 ± 18	56 ± 7	0.725 ± 0.004	...

[a] S denotes sharp component; B denotes broad component.

[b] Herbig 1960 data reanalyzed.

© American Astronomical Society • Provided by the NASA Astrophysics Data System

1980ApJ...240..871S

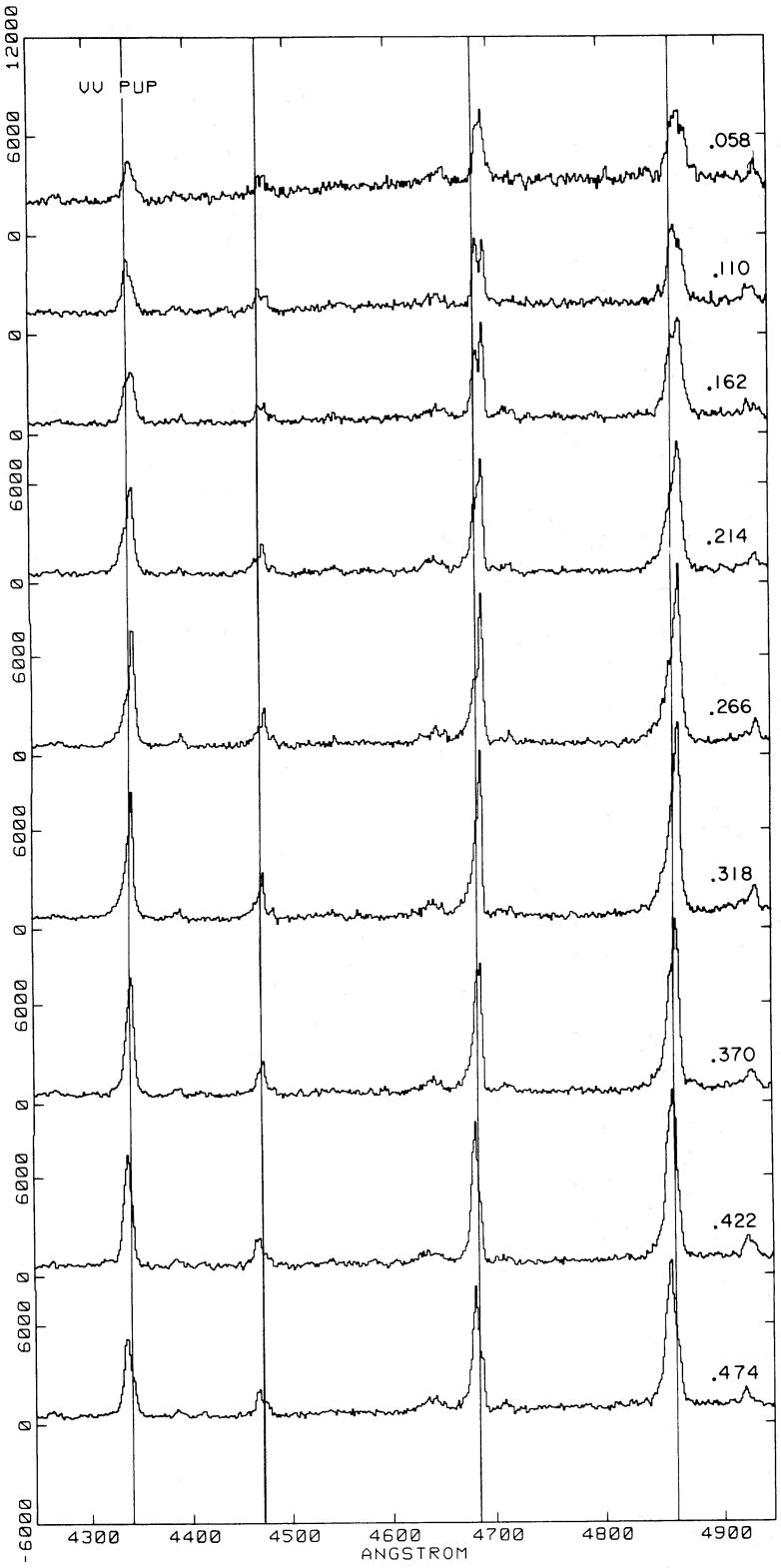

FIG. 4*a*

FIG. 4.—(*a*, *b*) A whole orbit of spectra of VV Pup. The data are plotted on identical linear vertical scales with various offsets to avoid confusion. The orbital phase of each spectrum is in the figure. The spectral resolution is 2.1 Å. The rest wavelengths of Hγ, He I λ4471, He II λ4686, and Hβ are depicted with long vertical lines (the apparent velocity of VV Pup due to terrestrial motion was $-19\,\mathrm{km\,s^{-1}}$ for the depicted orbit).

© American Astronomical Society • Provided by the NASA Astrophysics Data System

1980ApJ...240..871S

FIG. 4*b*

© American Astronomical Society • Provided by the NASA Astrophysics Data System

1980ApJ...240..871S

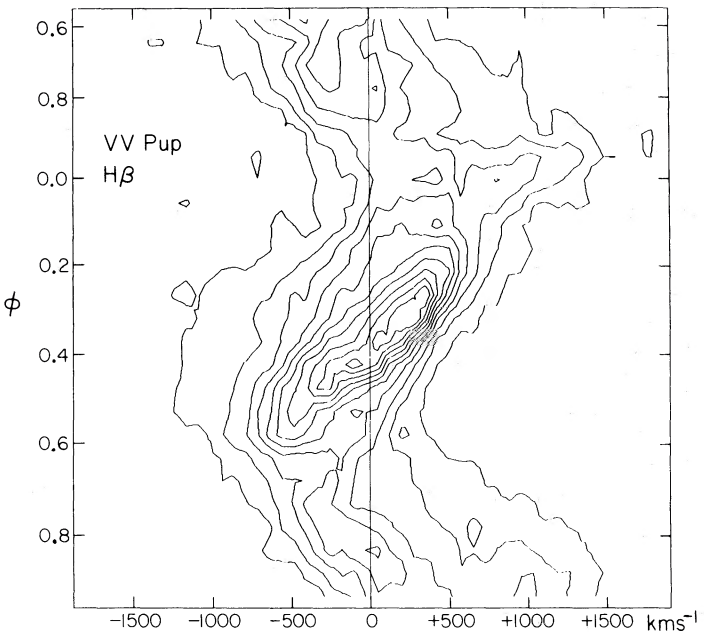

FIG. 5*a*

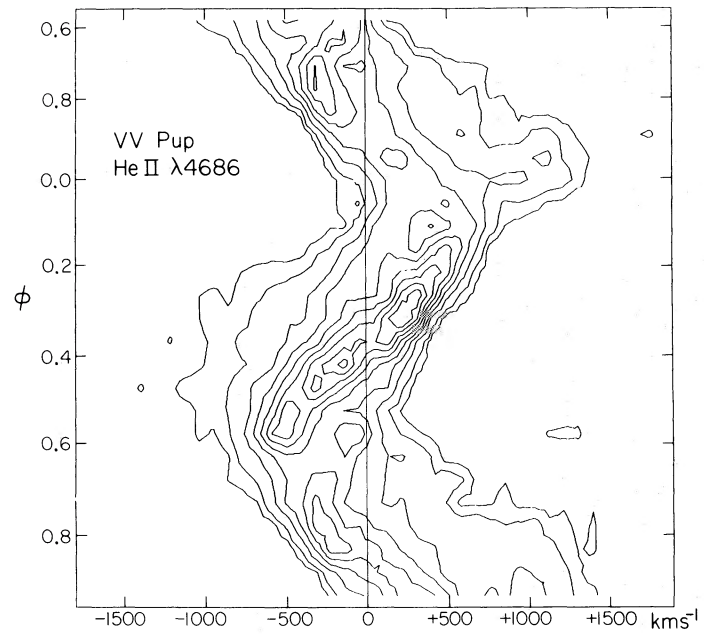

FIG. 5*b*

FIG. 5.—(*a*, *b*) Boroson-Greenstein diagrams for the Hβ and He II λ4686 emission lines in VV Pup. Twenty-six spectra taken consecutively have been used to create a contour plot of emission line strength in velocity space as the orbital phase ϕ varies. The continuum has been subtracted from each spectrum for the contouring. The velocity of VV Pup due to Earth's motion is -19 km s^{-1}.

phase with the main broad base in the line (as may be seen by inspecting Fig. 5). In order to quantify this effect we have measured the two components separately (denoted S for sharp and B for broad). Radial velocity parameters given in Table 3 show:

1. The B component has only a slightly larger K than the S component. The K-value for the S component in VV Pup is as high as 437 km s^{-1}, compared with 140 km s^{-1} in AM Her.

2. The γ-velocity for the B component is persistently redward of the S component γ-velocity.

3. The S and B components have a phase difference

© American Astronomical Society • Provided by the NASA Astrophysics Data System

1980ApJ...240..871S

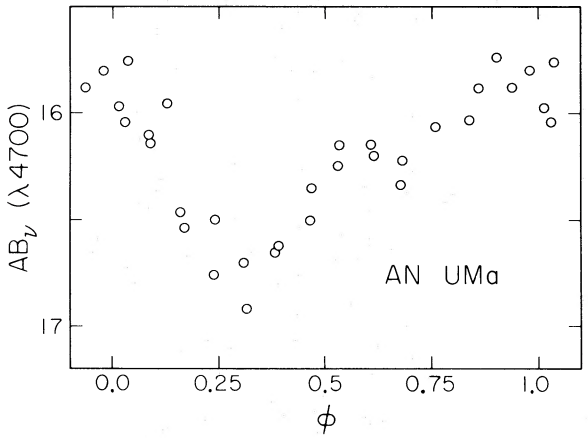

FIG. 6.—Light curve of AN UMa from Cassegrain slit photometry. The curve has been normalized with a total flux observation to give AB$_\nu$ at λ4700. Photometric phase ϕ from the standard ephemeris is the abscissa.

of 53°, compared with 133° for AM Her and 25° in 2A 0311−227.

There are other peculiarities seen by examining Figure 4. The emission lines become very fat at phase 0.9, and all lines exhibit duplicity. Additionally, the He II λ4686 line exhibits close duplicity at phases 0.1 and 0.6. Hints of this are seen in the Balmer lines which fail, however, to show the clean split shown by the He II λ4686 line.

IV. AN URSAE MAJORIS

a) *The Ephemeris*

All phases have been computed with the formula given to us by Tapia (1979, private communication).

$$\text{HJD} = 2443191.7879 + 0.07975307E\,, \qquad (6)$$

which gives the time of a linear polarization spike. Our light curve from Cassegrain slit photometry is in Figure 6 and may be compared with the light curve in Krzeminski and Serkowski (1977). The position of our primary minimum is at most 0.05 phases earlier than theirs, indicating only slight, if any, phase slippage from equation (6). We shall thus compute all phases from equation (6).

Our radial velocity epoch (for $V = \gamma$ crossing from blue to red) is

$$\text{HJD} = 2444217.99612 \pm 0.00072\,, \qquad (7)$$

which gives a fiducial phase,

$$\phi_0 = 0.319 \pm 0.009\,, \qquad (8)$$

for the mean positions of the emission lines.

b) *Emission Line Behavior*

Figure 7 shows an orbital period of AN UMa depicted in 13 consecutive spectra. Data from the two orbits we observed have been melded together (two observations per spectrum in the figure) in order to improve the less than impressive signal-to-noise ratio. Various features then become clear, notably the development of a fat blue wing at $\phi = 0.8$ and fat red wing at $\phi = 0.2$ in the emission lines. This sort of behavior (also seen in 2A 0311−227; see SY) is caused by (*a*) the line base and peak being slightly out of phase, and (*b*) a lower *K*-velocity for the peak than for the base.

This effect appears to be operating in AN UMa, as may be seen by inspecting the radial velocity fits in Table 4. Here, however, it is more the de-phased motion (peak lags base by 49°) than the slight but significant difference in *K* velocities that causes the "swing-wing" effect. Further, as may be seen by inspecting Figure 4, the lines have a modest flux minimum at $\phi = 0.3$. The changes are minor compared with those in VV Pup where components leap up

TABLE 4

RADIAL VELOCITIES IN AN URSAE MAJORIS

Line[a]	K (km s^{-1})	γ (km s^{-1})	ϕ_0	$\sigma(O-E)$ (km s^{-1})
Hγ	266 ± 22	−47 ± 17	0.311 ± 0.014	87
He I λ4471	259 ± 32	−65 ± 24	0.308 ± 0.021	127
He II λ4686	262 ± 25	−33 ± 19	0.322 ± 0.016	99
Hβ	236 ± 27	−41 ± 20	0.337 ± 0.020	107
Mean	256 ± 13	−47 ± 10	0.319 ± 0.009	...
Hγ (P)	250 ± 55	−36 ± 44	0.357 ± 0.035	142
He II λ4686 (P)	279 ± 58	−44 ± 47	0.380 ± 0.027	149
Hβ (P)	283 ± 44	−38 ± 35	0.392 ± 0.024	111
Mean (P)	271 ± 31	−39 ± 24	0.376 ± 0.016	...
Hγ (B)	321 ± 26	−56 ± 21	0.244 ± 0.013	65
He II λ4686 (B)	326 ± 37	−31 ± 30	0.224 ± 0.018	94
Hβ (B)	320 ± 29	−40 ± 23	0.251 ± 0.014	74
Mean (B)	322 ± 17	−42 ± 14	0.240 ± 0.009	...

[a] Line peak denoted by P; base by B.

© American Astronomical Society • Provided by the NASA Astrophysics Data System

1980ApJ...240..871S

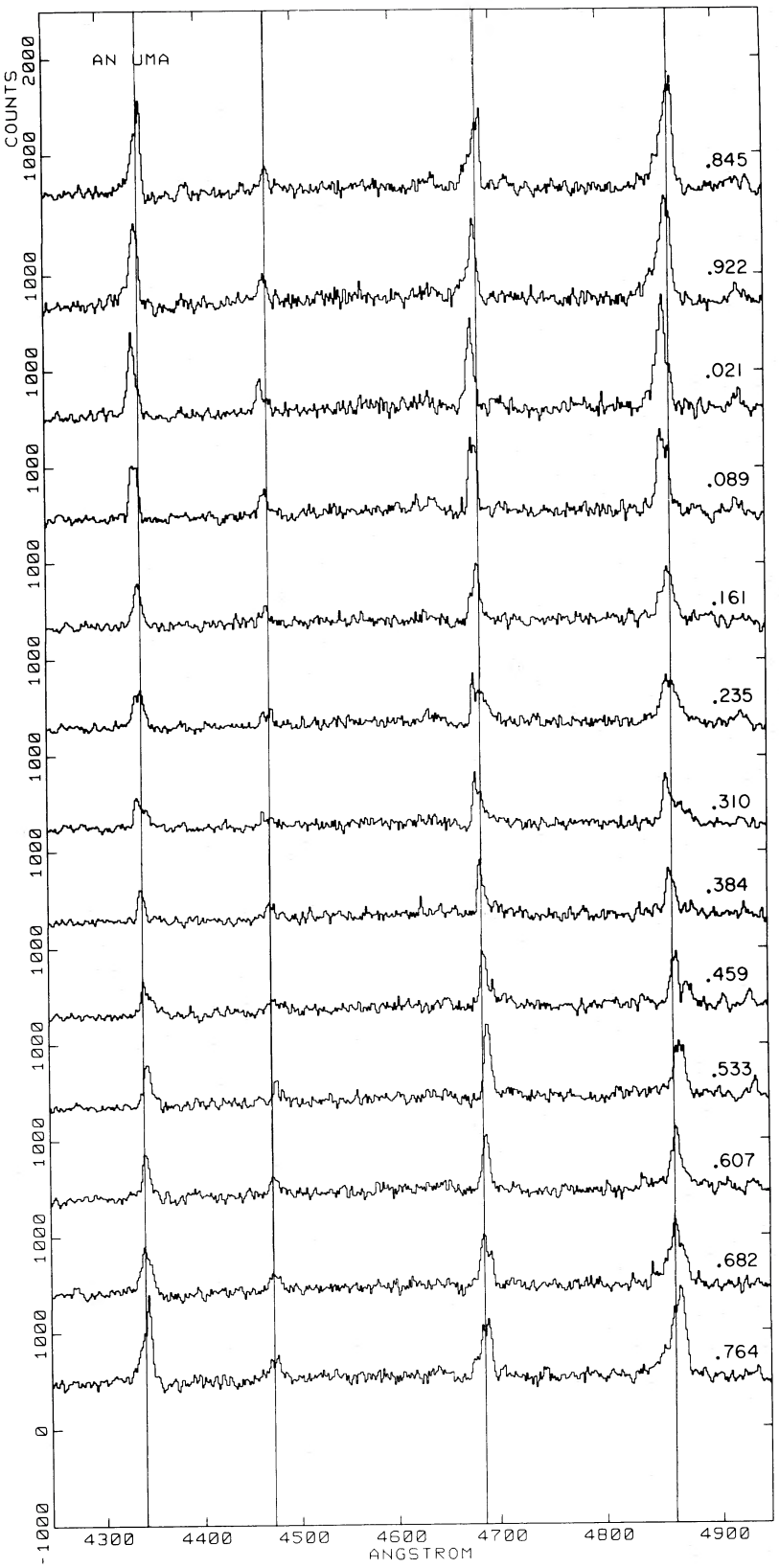

FIG. 7.—An entire orbit of spectra of AN UMa. Other notes as for Fig. 4 (except terrestrial motion is $-22\ \mathrm{km\ s^{-1}}$).

© American Astronomical Society • Provided by the NASA Astrophysics Data System

1980ApJ...240..871S

and down with wild abandon. There is, further, no striking sharp component of the type possessed by both VV Pup and AM Her. 2A 0311−227 also lacks a sharp component. A subdued version of such a component manifests itself at $\phi = 0.7$, moves sedately to the blue, and disappears at $\phi = 0.1$.

V. DISCUSSION

a) *Kinematics of Accretion Stream*

In SY, initial exploration of a kinematical model for an accretion stream in 2A 0311−227 was described. This type of model was initially proposed for VV Pup by Liebert *et al.* (1978). In this model a synchronously locked white dwarf star with dipole magnetic field is assumed to exist. The field threads gas exuded by the red dwarf near the L_1 point. The gas flows along magnetic field lines and plummets onto the magnetic pole of the white dwarf.

In the Roche geometry suppose that the white dwarf's dipole field points along the rotation axis of the binary. If material is threaded on the field lines near L_1, it must proceed initially vertically out of the orbital plane. This it cannot do freely since it must climb out of the Roche potential until the field lines become tangent to the potential surface when it may cruise freely down the potential well. The polarization variations and eclipses in magnetic binaries indicate inclined dipoles. If the dipole is cocked by more than 16° (essentially independent of mass ratio), then one pole becomes accessible to liberated gas while the other pole remains starved.

Consider the geometry outlined in SY with dipole angles ϕ_* and ψ_* as defined there. Let the star masses by m_W (white dwarf), m_R (red dwarf), and the mass ratio $q = m_W/m_R$. In the dipole geometry material at angle θ in the coordinates defined by SY is at position

$$\boldsymbol{x} = r(\sin\theta, \cos\theta \sin\psi_*, \cos\theta\cos\psi_*) . \quad (9)$$

When threaded on the field line passing through the L_1 point $\boldsymbol{x}_L = (x_L, 0, 0)$, the distance from the white dwarf is

$$r = x_L \sin^2(\theta - \theta_*) \sec^2\theta_* . \quad (10)$$

Note that we shall measure all distances in terms of the binary separation (a). The dimensionless potential [its units are in terms of $G(m_R + m_W)/a$] is

$$\psi(\boldsymbol{x}) = -(q/1+q)/r - (1/1+q)/r' - p^2/2 , \quad (11)$$

where r' = distance from red star and p = distance from rotation axis.

Material threaded on a sufficiently sturdy magnetic field line will ignore the Coriolis force (as it acts perpendicular to the direction of motion), and the material will have a velocity

$$v = (\psi_L - \psi)^{1/2} , \quad (12)$$

where $\psi_L = \psi(\boldsymbol{x}_L)$ and assuming $v = 0$ for $\boldsymbol{x} = \boldsymbol{x}_L$. Defining

$$v_0^2 = v^2[4\cos^2(\theta - \theta_*) + \sin^2(\theta - \theta_*)]^{-1} ,$$
$$v_x = v_0 \sin(\theta - \theta_*)\cos\theta + 2v_0\cos(\theta - \theta_*)\sin\theta ,$$
$$v_z = 2v_0\cos(\theta - \theta_*)\cos\theta - v_0\sin(\theta - \theta_*)\sin\theta , \quad (13)$$

we find the gas velocity to be given by (including the orbital motion)

$$u_x = -v_x - y , \quad u_y = -v_z \sin\psi_* + x - 1/(1+q) ,$$
$$u_z = -v_z\cos\psi_* . \quad (14)$$

The unit vector toward Earth is

$$\boldsymbol{n} = (\sin i\cos 2\pi\phi, \ -\sin i \sin 2\pi\phi, \cos i) \quad (15)$$

for binary phase $\phi \in [0, 1)$ with $\phi = 0$ for inferior conjunction of the red dwarf.

The observed velocity of $-\boldsymbol{u}\cdot\boldsymbol{n}$ gives radial velocity parameters,

$$K = \{u_x^2 + u_y^2\}^{1/2}\sin i , \quad \gamma = -u_z\cos i ,$$
$$\phi_0 = \mathrm{ATAN2}(u_x, u_y)/2\pi , \quad (16)$$

where $\mathrm{ATAN2}(u_x, u_y)$ is the 4-quadrant inverse tangent $\tan^{-1}(u_x/u_y)$.

A unit vector along the accreting magnetic pole is

$$\boldsymbol{d} = (\sin\theta_*, \cos\theta_*\sin\psi_*, \cos\theta_*\cos\psi_*) , \quad (17)$$

so the angle between pole and Earth is

$$\cos\theta_D = \boldsymbol{d}\cdot\boldsymbol{n} . \quad (18)$$

b) *Application to VV Puppis*

If the red star fills its Roche lobe,

$$(r_R/R_\odot)^3(m_R/M_\odot)^{-1} = 9.7842 \times 10^{-10} P^2 \quad (19)$$

for a system with period P seconds, assuming $q > 1$. A binary with a period as short as VV Pup has problems when one tries to fit a reasonable red star onto its Roche lobe. A mass-radius diagram (Young and Schneider 1979) reveals the star to be below the zero-age main sequence for any mass $m_R > 0.2\ M_\odot$. On the other hand, if $m_R < 0.2\ M_\odot$, the star's luminosity becomes insignificant. Yet the star may have been observed (Liebert *et al.* 1978), so let us *assume* $m_R = 0.2\ M_\odot$.

We are hampered in our analysis by not knowing the photometric phase of the red star conjunction. We are struck by the similarity in behavior of the "sharp" emission components in VV Pup and AM Her. Let us assume, therefore, that the sharp component arises on the exposed face of the red star as it does in AM Her (Young and Schneider 1979). This gives $K_R = 437\ \mathrm{km\ s^{-1}}$ and a mass function

$$f = m_W^3(m_W + m_R)^{-2}\sin^3 i = 0.606\ M_\odot . \quad (20)$$

We suspect that the inclination is quite high. This would explain the extreme variations in the strength of the sharp component in a manner entirely consistent

© American Astronomical Society • Provided by the NASA Astrophysics Data System

1980ApJ...240..871S

TABLE 5

VV PUPPIS: ACCRETION STREAM MODEL

Radius r	Angle θ	Velocity v	Area A/A_0	K	γ	ϕ_0[a]
0.00620	89.0964	16.418	8.02×10^{-7}	14.998	0.099	0.749
0.02480	89.1928	8.053	5.13×10^{-5}	7.357	0.041	0.747
0.05580	89.2892	5.190	5.85×10^{-4}	4.742	0.021	0.747
0.09920	89.3856	3.699	3.29×10^{-3}	3.379	0.011	0.748
0.15499	89.4820	2.749	1.25×10^{-2}	2.512	0.005	0.750
0.22319	89.5784	2.064	3.75×10^{-2}	1.886	0.002	0.755
0.30378	89.6748	1.520	9.44×10^{-2}	1.395	0.000	0.766
0.39677	89.7712	1.053	2.10×10^{-1}	0.988	−0.001	0.786
0.50215	89.8676	0.620	4.27×10^{-1}	0.650	−0.001	0.831
0.61993	89.9640	0.179	8.03×10^{-1}	0.456	0.000	0.942

NOTE.—$q = 5.5$, $i = 66°$, $\theta_* = 89°$, $\psi_* = 0°$, $x_L = 0.6671$, $K_R = 0.773$, $K_W = 0.141$. Dipole angles: 23° ($\phi = 0$), 90° ($\phi = 0.251$), 155° ($\phi = 0.5$), 90° ($\phi = 0.749$).

[a] In theoretical system where $\phi = 0$ for inferior conjunction of red dwarf.

with the emitting region being almost totally eclipsed by the red star. Values of $i = 66°$ and $m_W = 1.1\ M_\odot$ which satisfy equation (20) will be assumed.

The eclipse of the cyclotron radiation is very long, and we shall suppose (after Liebert *et al.* 1978) that it is obscured by the white dwarf itself. This will require a massive dipole inclination ($\sim 90°$ to the rotation axis of the system). In fact, a simple model with the dipole pointing straight at the red star does quite well. Parameters for the model are found in Table 5. The most critical parameter to fit is the perpendicularity of the accretion column near the magnetic pole. This occurs 0.24 of a phase after the red star conjunction (at $\phi = 0.12$ in the photometric system) when there is a linear polarization spike (Liebert *et al.* 1978). The eclipse starts at this time and lasts until photometric phase 0.65. The model in Table 5 has the dipole tucked away behind the white dwarf for half the orbit, as required by the length of the eclipse.

The phase of the broad lines is always 0.15–0.20 phases ahead of the sharp lines. This is very insensitive to the dipole inclination, or any of the model parameters unless drastic dipole angles are postulated.

This model (which we intend to be illustrative, not definite) has some difficulties. A dipole inclination of 90° gives an eclipse duration of 0.5, not 0.6 as observed. A closer inspection of the light curve (Fig. 3) indicates that while ingress is quite steep, egress is not as well defined. A more serious objection is polarization evidence of accretion onto both poles (Liebert and Stockman 1979). The double-lined nature of the emission at some phases is also suggestive of two accretion streams. If this were the situation, one would expect the peaks to be antiphased; the observations show they are phased. The polarization result is more difficult to refute; we note only that if the emission is reflected off the components and/or accretion column, the sign of the circular polarization will be reversed. A final point is the lack of a second polarization spike as the accreting pole emerges from eclipse; Stockman (1977) discusses this point. That these features are fickle is demonstrated by the disappearance of the primary linear polarization spike in AM Her itself!

c) *Application to AN Ursae Majoris*

In this object we are really thwarted by not knowing where the red star is. Unlike VV Pup, there is no obvious striking "sharp" component in the emission lines. A weak component of this nature may be seen, however, in Figure 6. It appears at $\phi = 0.7$, drifts blueward, and subsides at $\phi = 0.1$. This behavior is similar to that of VV Puppis but is much more sedate.

According to Krzeminski and Serkowski (1977) the circular polarization is always negative, and a fat linear polarization pulse is seen when the circular polarization is closest to zero. No eclipses seem to occur—an observation which suggests that the accreting pole is always in the hemisphere of the white dwarf facing Earth. It would, at its far point, be roughly perpendicular to the line of sight in order to create a fat linear polarization spike at $\phi = 0$.

This is consistent with some sort of model like that in Table 6. Here the broad component of the line has a maximum redshift when the dipole is pointed near Earth and a maximum blueshift when pointed farthest from Earth. At this time the dipole is nearly perpendicular to the line of sight and a linear polarization pulse ensues. The line peak is a combination of the gas at the top of the accretion column and irradiated photosphere from the red star and lags the broad component by ~ 0.15 phases.

Table 6 is not proffered as any sort of "solution" for AN UMa, merely as being indicative of the sort of emission line and dipole phasing that result in such an idealized geometry.

d) *The Accretion Flow*

We shall assume that the material threaded on magnetic field lines is cool and so its internal pressure is insufficient to prevent (supersonic) free-fall onto the

© American Astronomical Society • Provided by the NASA Astrophysics Data System

1980ApJ...240..871S

TABLE 6

AN URSAE MAJORIS: ACCRETION STREAM MODEL

Radius r	Angle θ	Velocity v	Area A/A_0	K	γ	ϕ_0[a]
0.00774	54.0	14.556	1.35×10^{-6}	7.08	6.27	0.784
0.03082	58.0	7.120	8.56×10^{-5}	3.64	2.57	0.775
0.06878	62.0	4.566	9.62×10^{-4}	2.44	1.31	0.768
0.12088	66.0	3.227	5.29×10^{-3}	1.78	0.68	0.763
0.18613	70.0	2.368	1.96×10^{-2}	1.33	0.31	0.760
0.26324	74.0	1.742	5.67×10^{-2}	0.99	0.08	0.761
0.35072	78.0	1.241	1.37×10^{-1}	0.70	−0.05	0.770
0.44687	82.0	0.807	2.92×10^{-1}	0.46	−0.10	0.796
0.54982	86.0	0.405	5.61×10^{-1}	0.29	−0.09	0.867
0.65757	89.9	0.004	9.95×10^{-1}	0.28	−0.00	0.998

NOTE.—$q = 5$, $i = 35°$, $\theta_* = 50°$, $\psi_* = -20°$, $x_L = 0.6586$, $K_R = 0.478$, $K_W = 0.096$. Dipole angles: 18° ($\phi = 0.045$), 88° ($\phi = 0.545$).

[a] In theoretical system where $\phi = 0$ for inferior conjunction of red dwarf.

white dwarf. The gas is clearly cool (~ 3000 K) as it wafts away from the red dwarf. While various ill-understood shocks and processes may heat the gas as it is field threaded, we point out that the deduced temperature from the Balmer line ratios is a paltry 10^4 K (Stockman *et al.* 1977). Note that the energy density in the magnetic field is $B^2/8\pi \sim 2 \times 10^3$ ergs cm^{-3} for a surface field of 2×10^8 gauss on a white dwarf of radius 10^9 cm (giving a field of 200 gauss near the L_1 point). The gaseous energy density $\rho c_s^2 \sim 20$ ergs cm^{-3} for a gas density $n_H = 10^{13}$ cm^{-3} and a sound speed 10 km s^{-1}. The gas would have to achieve a speed of 100 km s^{-1} for its ram energy density ρv^2 to compete with the magnetic energy density. It would easily be able to obtain such a speed by plunging away toward the white dwarf in the absence of a magnetic field. Channeled by the field, however, $\rho v^2 \propto r^{-7/2}$ and $B^2/8\pi \propto r^{-6}$, so that once the gas loses control, it stays lost.

There is strong evidence that the surface field on VV Pup is substantially lower than the value used in the above calculation (3×10^7 gauss, Stockman, Liebert, and Bond 1979; Visvanathan and Wickramasinghe 1979). This would make the gas energy density much more competitive with the field, although it is not clear which is greater.

The area of a funnel defined by a set of field lines varies as

$$A = r^3[\sin^2(\theta - \theta_*) + 4\cos^2(\theta - \theta_*)]^{-1/2} . \quad (21)$$

Since we are near the axis ($\theta - \theta_*$) of the dipole, we shall take

$$A = A_0(r/r_0)^3 , \quad (22)$$

where A_0 is the area of the funnel mouth in the vicinity of the L_1 point.

The funnel must have a wide mouth. Its surface area as seen from the side would be

$$S = \tfrac{4}{5} r_0 (A_0/\pi)^{1/2} . \quad (23)$$

Now the Balmer lines are optically thick and characterized by a temperature $\sim 10^4$ K (see Liebert *et al.* 1978) and require a surface area of $\sim 4 \times 10^{20} (D/100 \text{ pc})^2$ cm^2 to attain the observed flux in VV Pup. The binary separation is $a = 5.4 \times 10^{10}$ cm, so the funnel length $r_0 = x_L a = 3.6 \times 10^{10}$ cm. Thence

$$(A_0/\pi)^{1/2} \sim 1.4 \times 10^{10} (D/100 \text{ pc})^2 \text{ cm} , \quad (24)$$

indicating that the maw is wide near the red dwarf. The red star may have to expand slightly beyond the critical Roche potential in order to fuel such a funnel.

The flow yields most of the line flux at $K = 1$ in Table 5, where $A/A_0 = 0.21$ and $v = 1 = 560$ km s^{-1}. If the output luminosity scales like AM Her, then the required accretion rate to account for such luminosity is

$$\dot{M} = 2.5 \times 10^{-11} (D/100 \text{ pc})^2 \quad (M_\odot \text{ yr}^{-1}) \quad (25)$$

for a white dwarf of radius 10^9 cm. The baryon flux is thus

$$\dot{N} = 9.4 \times 10^{38} (D/100 \text{ pc})^2 \quad (\text{baryons s}^{-1}) . \quad (26)$$

From the conservation equation,

$$\dot{N} = nAv \quad (27)$$

at all points in the funnel. Thus where the line flux emerges, $A \sim 1.3 \times 10^{20} (D/100 \text{ pc})^4$, and thus $n \sim 1.5 \times 10^{11} (D/100 \text{ pc})^{-2}$ (baryons cm^{-3}). The limit $n_e > 10^{12}$ cm^{-3} (Liebert *et al.* 1978) was obtained by considering free-bound emission from a spherically symmetric, homogeneous medium. In fact, the free-bound Balmer emission probably comes from farther down the funnel than the line flux. This is because the emission is

$$\varepsilon_{fb}(r)dr = Cn(r)^2 A(r) T(r)^{-3/2} dr ; \quad (28)$$

and since $A \propto r^3$, $n(r) \propto r^{-5/2}$ [since $v(r) \propto r^{-1/2}$];

© American Astronomical Society • Provided by the NASA Astrophysics Data System

1980ApJ...240..871S

thus $\varepsilon_{fb}(r) \propto r^{-2} T(r)^{-3/2}$. The temperature $T(r)$ is difficult to evaluate since it would require careful integration of the gaseous heat-balance equations as the tortured gas takes the big dive.

We would like to thank Santiago Tapia for communicating his polarization results prior to publication, Bruce Cuney for assistance at the 5 meter, and Barbara Zimmerman for aid in data reduction.

REFERENCES

Bond, H. E., and Wagner, R. L. 1977, *IAU Circ.*, No. 3049.
Greenstein, J. L., Sargent, W. L. W., Boroson, T. A., and Boksenberg, A. 1977, *Ap. J. (Letters)*, **218**, L121.
Herbig, G. H. 1960, *Ap. J.*, **132**, 76.
Krzeminski, W., and Serkowski, K. 1977, *Ap. J. (Letters)*, **216**, L45.
Liebert, J., and Stockman, H. S. 1979, *Ap. J.*, **229**, 652.
Liebert, J., Stockman, H. S., Angel, J. R. P., Woolf, N. J., Hege, K., and Margon, B. 1978, *Ap. J.*, **225**, 201.
Schneider, D. P., and Young, P. 1980, *Ap. J.*, **238**, 946 (SY).
Stockman, H. S. 1977, *Ap. J. (Letters)*, **218**, L57.
Stockman, H. S., Liebert, J., and Bond, H. E. 1979, in *IAU Colloquium 53* (Rochester: University of Rochester), p. 334.
Stockman, H. S., Schmidt, G. D., Angel, J. R. P., Liebert, J., Tapia, S., and Beaver, E. A. 1977, *Ap. J.*, **217**, 815.
Tapia, S., 1977*a*, *IAU Circ.*, No. 3049.
———. 1977*b*, *IAU Circ.*, No. 3054.
Visvanathan, N., and Wickramasinghe, D. T. 1979, in *IAU Colloquium 53* (Rochester: University of Rochester), p. 330.
Walker, M. F. 1965, *Mitt. Sternw. Budapest*, No. 57.
Warner, B., and Nather, R. E. 1972, *M.N.R.A.S.*, **156**, 305.
Young, P., and Schneider, D. P. 1979, *Ap. J.*, **230**, 502.

DONALD P. SCHNEIDER and PETER YOUNG: Department of Astronomy 105-24, California Institute of Technology, Pasadena, CA 91125

© American Astronomical Society • Provided by the NASA Astrophysics Data System